Acta Crystallographica Section D
Biological Crystallography
ISSN 0907-4449

The catalytic module of Cel7D from *Phanerochaete chrysosporium* as a chiral selector: structural studies of its complex with the beta blocker (*R*)-propranolol

Inés G. Muñoz, Sherry L. Mowbray and Jerry Ståhlberg*

Department of Molecular Biology, Swedish University of Agricultural Sciences, Biomedical Centre, PO Box 590, SE-751 24 Uppsala, Sweden

Correspondence e-mail: jerry.stahlberg@molbio.slu.se

Received 12 August 2002
Accepted 21 January 2003

PDB Reference: Cel7D catalytic domain, 1h46, r1h46sf.

Previous investigations have shown that the major cellobiohydrolase of *Phanerochaete chrysosporium*, Cel7D (CBH 58), can be used to separate the enantiomers of a number of drugs, including adrenergic beta blockers such as propranolol. The structural basis of this enantioselectivity is explored here. A 1.5 Å X-ray structure of the catalytic domain of Cel7D in complex with (*R*)-propranolol showed the ligand bound at the active site in glucosyl-binding subsites −1/+1. The catalytic residue Glu207 makes a strong charge–charge interaction with the secondary amine of (*R*)-propranolol; this is supported by a second interaction of the amine with the nearby Asp209. The aromatic naphthyl group stacks onto the indole ring of Trp373 (normally the glucosyl-binding platform of subsite +1). Other factors also contribute to good complementarity between the ligand and the substrate-binding cleft of the enzyme. Comparison with the previous structure of a related cellulase, Cel7A from *Trichoderma reesei*, in complex with (*S*)-propranolol strongly suggests that these enzymes will bind the (*S*)-enantiomer in a very similar manner, distinct from their mode of binding to (*R*)-propranolol. Tighter binding of both enzymes to the (*S*)-enantiomer is largely explained by two additional hydrogen-bonding interactions with its hydroxyl group. The distinct preference for the (*R*)-enantiomer is probably a consequence of structural differences near the naphthyl group of the ligand.

1. Introduction

Cellobiohydrolase Cel7D (previously called CBH 58) is the major cellobiohydrolase produced by the basidiomycete *Phanerochaete chrysosporium* under most growth conditions (Eriksson & Pettersson, 1975). In structure and function, it is similar to the well characterized cellobiohydrolase of *Trichoderma reesei*, Tr_Cel7A (formerly called CBH 1). Like many other cellulases, these enzymes are composed of two functional units, a cellulose-binding module and a catalytic module, which are connected by a highly glycosylated linker peptide. Using nomenclature based on the catalytic modules (Henrissat *et al.*, 1998), they have been assigned to family 7 of the glycosyl hydrolases (Henrissat & Bairoch, 1996; Henrissat & Davies, 1997) and, like all family members tested to date, cleave the β-1,4-glycosidic bond with net retention of the anomeric carbon configuration (Gebler *et al.*, 1992). Cellobiohydrolases belonging to family 7 are thought to act processively from the reducing end of cellulose chains, generating β-cellobiose as the main product (Barr *et al.*, 1996; Boisset *et al.*, 2000; Divne *et al.*, 1998). The family also includes

some members which act as endoglucanases; that is, they make internal cuts within the cellulose chain.

The structure of the catalytic module of Tr_Cel7A is known (Divne *et al.*, 1994) and we have recently published the structure of the equivalent module of Pc_Cel7D (Muñoz *et al.*, 2001). Each has a primary fold consisting of two β-sheets that pack face-to-face to form a β-sandwich. Structures of Tr_Cel7A in complex with various sugars have investigated its active site in detail (Divne *et al.*, 1998; Ståhlberg *et al.*, 1996). A cellulose-binding tunnel extends ~50 Å along the concave surface of one of its β-sheets and is largely enclosed by loops protruding from the β-sandwich. Tr_Cel7A binds ten glucosyl units in subsites −7 to +3 (numbering starts from the point of glycosidic bond cleavage, between −1 and +1, with negative numbers indicating the non-reducing end of the cellulose chain and positive numbers the reducing end; Davies *et al.*, 1997). Three acidic residues (Glu212, Asp214 and Glu217) are responsible for cleavage of the cellulose chain. Superposition of the structure of Tr_Cel7A onto that of Pc_Cel7D shows that most aspects of substrate binding and catalysis are conserved (Muñoz *et al.*, 2001). In Pc_Cel7D there is an extra aromatic residue at the entrance of the tunnel, Tyr47, which forms a potential −8 subsite. Partial deletion of three loops extending from the β-sandwich converts the tunnel into a more open cleft in Pc_Cel7D. Three carboxylate residues (Glu207, Asp209 and Glu212) comprise a catalytic site equivalent to that of Tr_Cel7A. The role of Glu207 is to act as a nucleophile and attack the anomeric carbon at the scissile bond and form a covalent glycosyl ester bond to the cleaved cellulose chain, which results in a glycosyl-enzyme intermediate. Glu212 is the catalytic acid/base. It acts as an acid in the first step of the reaction and protonates the glycosidic oxygen, while in the second step Glu212 acts as a base and abstracts a proton from a water molecule that attacks and cleaves the glycosyl-enzyme intermediate. Asp209 is hydrogen bonded to the catalytic nucleophile Glu207 (Muñoz *et al.*, 2001). The corresponding residue in Tr_Cel7A has been shown to be important for catalytic activity (Ståhlberg *et al.*, 1996). It most certainly influences the charge distribution at the cleavage site, but its exact role is uncertain.

Cellulases such as Pc_Cel7D and Tr_Cel7A have attracted substantial interest with regard to a number of actual and potential industrial applications. One of these derives from the observation that the enzymes can discriminate between the enantiomers of a number of pharmaceutically active compounds (Henriksson *et al.*, 2000; Isaksson *et al.*, 1994; Marle *et al.*, 1991). This is of significant medical interest, since only one enantiomer generally possesses the desired activity; the other can actually cause unwanted side effects. Enantiomeric separations using cellulases have been carried out in two different ways: (i) with a chiral stationary phase, in which intact or fragmented enzyme was covalently attached to silica (Aboul-Enein & Serignese, 1997; Götmar *et al.*, 2001; Marle *et al.*, 1993), and (ii) in high-performance capillary electrophoresis, using the enzyme in either the mobile or stationary phase (Haginaka, 2000; Hedeland, Nygard *et al.*, 2000). Enantioseparation was found to be strongly dependent on pH, ionic strength, temperature and the presence of charged or uncharged modifiers in the mobile phase. Both the catalytic and the cellulose-binding modules of Tr_Cel7A actually possess enantioselectivity, but the major source of chiral recognition lies within the catalytic module (Marle *et al.*, 1993). A Tr_Cel7A–silica column is in use commercially under the trade name CHIRAL-CBH (ChromTech AB, Sweden).

Tests of Pc_Cel7D in silica-based liquid-chromatographic separations (Henriksson *et al.*, 2000) have proved it to have higher enantioselectivity than Tr_Cel7A for more hydrophilic compounds such as atenolol and metoprolol. Both enzymes gave good chiral separation of β-adrenergic antagonists, while neither was useful for resolving any of the acidic compounds tested. Solutes were retained longer on the Pc_Cel7D phase in general, suggesting that it has greater potential for applications in bioanalysis. The same study showed that chiral analytes function as competitive inhibitors, suggesting that they would bind in the active site. Cellobiose or lactose (inhibitors which bind in the +1,+2 site) interfered with enantioselectivity when added to the mobile phase, further indicating an overlap of the enantioselective and catalytic sites. This was confirmed by the recent structure of Tr_Cel7A in complex with (*S*)-propranolol: the drug bound at the active site with its amino group interacting directly with two catalytic acid residues (Ståhlberg *et al.*, 2001).

In the present report, we present the structure of the catalytic module of Pr_Cel7D in complex with (*R*)-propranolol refined at 1.52 Å resolution. This structure leads to a deeper understanding of the modes of binding and basis for enantioselectivity in this family of enzymes.

Table 1
Data-collection and refinement statistics for the (*R*)-propranolol complex.

Data collection	
Environment	CCD detector, ESRF, beamline ID14-4
Wavelength (Å)	0.9392
Unit-cell parameters (Å, °)	a = 86.1, b = 46.6, c = 98.8, β = 103.0
Space group	*C*2
Resolution† (Å)	48.22–1.52 (1.60–1.52)
Unique reflections	58656
Average multiplicity	4.8
Completeness	100 (100)
$R_{\rm merge}$†‡	0.085 (0.405)
$\langle I/\sigma(I^2I)\rangle$†§	10.0 (4.4)
Refinement	
No. of reflections used	55639
Completeness (%)	99.8
Resolution range (Å)	40.0–1.52
R factor/$R_{\rm free}$ (%)	16.7/21.6
No. of protein atoms (average B, Å^2)¶	3198 (22.2)
No. of water molecules (average B, Å^2)¶	333 (33.2)
No. of carbohydrate atoms (average B, Å^2)¶	14 (32.4)
No. of ligand atoms (average B, Å^2)¶	19 (34.9)
R.m.s bond length (Å)	0.009
R.m.s. bond angle (°)	1.6
No. of Ramachandran plot outliers†† (percentage)	3 (0.8)

† Values for the highest resolution shell are given in parentheses. ‡ $R_{\rm merge} = \sum_h \sum_i |I_{h,i} - \langle I_h\rangle| / \sum_h \sum_i |I_{h,i}|$. § Taken from *TRUNCATE* (French & Wilson, 1978). ¶ Calculated using *MOLEMAN* (Kleywegt, 1997). †† A stringent-boundary Ramachandran plot was used (Kleywegt & Jones, 1996).

2. Experimental

2.1. Protein preparation, crystallization and data collection

Preparation of the deglycosylated catalytic module of Cel7D from *P. chrysosporium* has been described previously (Muñoz *et al.*, 2001). Hanging-drop vapour-diffusion experiments included 18 mg ml^{-1} protein, 100 m*M* Tris–HCl pH 7.0, 5 m*M* Ca_2Cl, 22.5% polyethylene glycol 5000 and 12% glycerol. Co-crystallization was performed in the presence of (*R*)- or (*S*)-propranolol (Sigma, St Louis, USA) at estimated final concentrations of 12.5 and 10 m*M*, respectively, which were the highest ligand concentrations attainable before precipitation occurred in the crystallization drops. Complete X-ray diffraction data sets were collected from single crystals using synchrotron radiation at beamlines X-11 at EMBL-DESY, Hamburg, ID14-EH4 at ESRF, Grenoble and I-711 at MAX-Lab, Lund. Statistics for the crystallographic data for the (*R*)-propranolol complex are summarized in Table 1. Five structures were also obtained by co-crystallization in the presence of (*S*)-propranolol, in which density for the protein was comparable to that of the (*R*)-propranolol complex but there was no detectable density for the ligand.

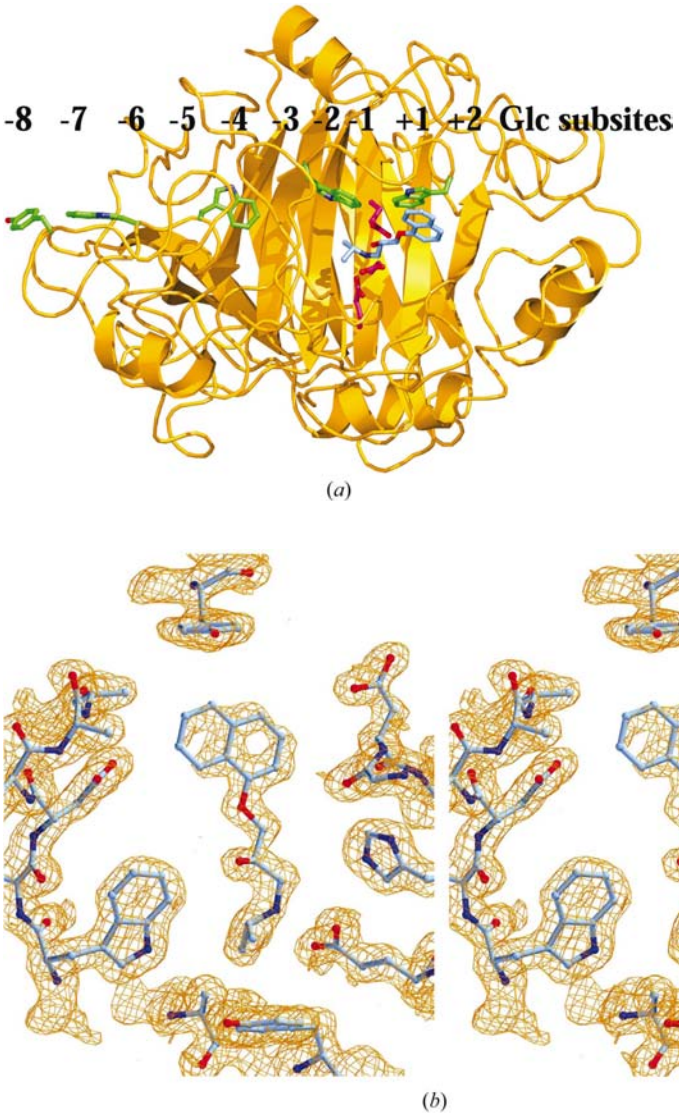

Figure 1
Binding of (*R*)-propranolol to Pc_Cel7D. (*a*) The main-chain structure of Pc_Cel7D is illustrated in gold, with the subsites of the cellulose-binding cleft numbered beginning with −8 at the non-reducing end of the cellulose chain. A ball-and-stick representation of (*R*)-propranolol is coloured light blue. Residues of the catalytic site are shown in red, while the aromatic residues that form the glucosyl-binding platforms of the various subsites are shown in green. (*b*) Electron density at the binding site for (*R*)-propranolol. $2F_o - F_c$ omit map, contoured at 1σ within 1.8 Å of the shown atom objects. The map was calculated using a protein model without ligand atoms included that had undergone five cycles of *REFMAC*5.0 refinement. Shown in divergent stereo.

2.2. Structure solution, model building, refinement and analysis of a complex with (*R*)-propranolol

5% of the reflections from this data set were set aside for free *R*-factor calculations (Brünger, 1992; Kleywegt & Brünger, 1996) during refinement. Initial phases were obtained using *CCP*4 (Collaborative Computational Project, Number 4, 1994) using the protein coordinates for apo Pc_Cel7D (PDB code 1gpi; Muñoz *et al.*, 2001). Refinement was carried out with *REFMAC*5 (Murshudov *et al.*, 1997, 1999) and included rigid-body refinement as the first step. As with previous data sets, the complex data were rather anisotropic and the most successful refinement strategy made use of Babinet's bulk-solvent correction (Moews & Kretsinger, 1975) combined with individual anisotropic temperature-factor refinement. Several rounds of rebuilding using the program *O* (Jones *et al.*, 1991) and the placement of water, a covalently bound residue of *N*-acetylglucosamine and (*R*)-propranolol into the electron density resulted in a model with an *R* factor of 16.7% and an $R_{\rm free}$ of 21.5%. Statistics after crystallographic refinement of this complex at 1.52 Å resolution are summarized in Table 1. Coordinates for the final model and the corresponding structure-factor data have been deposited in the PDB (Berman *et al.*, 2000) with entry code 1h46. Structures were aligned and compared using the programs *LSQMAN* (Kleywegt, 1996) and *O* (Jones *et al.*, 1991). The figures were prepared using *O*, *Molray* (Harris & Jones, 2001), *POVRay* (http://www.povray.org) and *MegaPOV* (http://nathan.kopp.com/patched.htm).

3. Results and discussion

3.1. Overall structure

Deglycosylated Pc_Cel7D catalytic module was crystallized in the presence of two different additives, (*S*)-propranolol and (*R*)-propranolol, each at a concentration expected to give high occupancy. The crystals were isomorphous with previous crystals (Muñoz *et al.*, 2001); all yielded strong diffraction data to beyond 2 Å resolution and allowed refinement of structures with well defined electron density for the protein. However, with (*S*)-propranolol, there was

no evidence of a bound ligand molecule anywhere in the binding cleft, despite numerous trials.

Convincing electron density was found for (*R*)-propranolol and a complex structure was refined at 1.52 Å resolution. Statistics relating to the diffraction data and the final refined model are summarized in Table 1. The model contains the complete catalytic module of Pc_Cel7D (residues 1–431), an *N*-acetylglucosamine residue bound to Asn286, a molecule of (*R*)-propranolol and 333 water molecules. The side chains of all amino acids in the active site could be positioned unambiguously. The protein molecule is essentially identical to the published structure of Pc_Cel7D (PDB code 1gpi; Muñoz *et al.*, 2001) with an overall r.m.s. difference of 0.1 Å when all C^{α} atoms are compared. The same artificial dimer in the crystal is present, with four residues at the C-terminus (427–430) forming an antiparallel β-strand interaction with the same four residues of a crystallographic symmetry-related molecule.

3.2. Binding of (*R*)-propranolol to Pc_Cel7D

The electron density clearly places the (*R*)-enantiomer of propranolol in subsites −1/+1 of Pc_Cel7D, interacting with the enzyme's catalytic residues (Fig. 1). Binding at this position provides an excellent explanation of why (*R*)-propranolol is an inhibitor of Pc_Cel7D and of why cellobiose and lactose, which inhibit Pc_Cel7D activity by binding in the +1, +2 sites, interfere with the binding of propranolol (Henriksson *et al.*, 2000).

The interactions between (*R*)-propranolol and Pc_Cel7D are illustrated in Fig. 2(*a*). Charge–charge interactions are observed between the secondary amino group of the ligand (pK_a = 9.5; Moffat *et al.*, 1986; pH of crystallization is 7.0) and Glu207 and Asp209. The distance to Glu207 (the nucleophile in catalysis) is short (2.6 Å) and suggests a particularly strong interaction. The alcohol group of propranolol hydrogen bonds only to a water molecule, while the ether O atom has no apparent hydrogen-bonding partner. Hydrophobic interactions between the naphthyl moiety of propranolol and the side chains of Trp373 (which forms the glucosyl-binding platform of subsite +1), Ala369, Tyr378 and others will also contribute significantly to binding. In addition, the methyl groups of the ligand make a number of van der Waals interactions with residues near the catalytic groups, notably Tyr142.

Density is weaker for the naphthyl moiety than for the rest of the ligand molecule (Fig. 1*b*). This is reflected in successively higher temperature factors on going from the amino-alcohol side chain (∼30 $Å^2$) towards the 'upper' edge of the naphthyl group (∼45 $Å^2$). The temperature factors of nearby side chains are also above the average in the binding-site cleft. For example, the side-chain atoms of Trp373, onto which the naphthyl group stacks, have temperature factors in the range 25–33 $Å^2$, whereas those for other side chains of the substrate-binding cleft are ∼20 $Å^2$. A plausible physical interpretation would be that the naphthyl end of the ligand is wobbling within the binding site and that this is accompanied by some movements of residues in the vicinity.

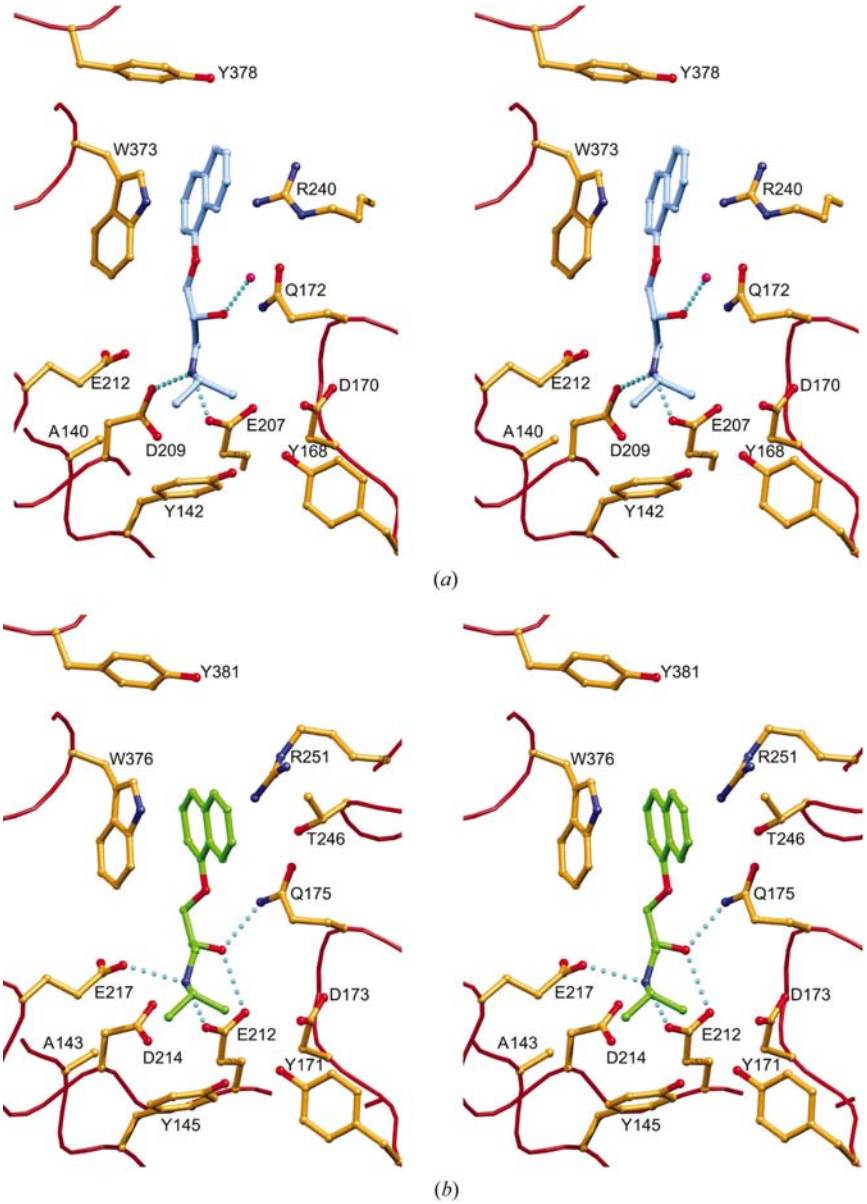

Figure 2
Interactions of Cel7 enzymes with propranolol enantiomers. (*a*) The complex of Pc_Cel7D with (*R*)-propranolol (atomic colours, with C atoms in light blue). (*b*) The complex of Tr_Cel7A with (*S*)-propranolol (green C atoms; PDB code 1dy4; Ståhlberg *et al.*, 2001). Both (*a*) and (*b*) are shown in divergent stereo. The side chains of a number of binding-site residues are shown in atomic colours (C atoms in gold) and hydrogen bonds with the ligands are indicated by cyan dotted lines. An interacting water molecule is represented as a red sphere.

3.3. Comparison with (*S*)-propranolol bound to *T. reesei* Cel7A

The structure of Tr_Cel7A bound to the (*S*)-enantiomer of propranolol (PDB code 1dy4; Ståhlberg *et al.*, 2001) provides information complementary to the present complex. The two enzymes are related closely enough to allow similarities and differences to be assessed with confidence (55% amino-acid sequence identity, r.m.s. difference of 0.9 Å for 411 matching C^{α} atoms); they are extremely similar in the immediate region of the catalytic residues.

In agreement with our earlier predictions (Henriksson *et al.*, 2000), these enzymes bind the respective enantiomers in analogous although not identical ways. Both inhibitors are bound in the −1 and +1 glucosyl-binding subsites. The details of interactions between (*S*)-propranolol and Tr_Cel7A are illustrated in Fig. 2(*b*). The main determinants of binding are the same as those described above, *i.e.* charge–charge interactions between the catalytic carboxylate residues and the propranolol amino group are accompanied by planar stacking interactions between the naphthyl moiety and the side chain of the tryptophan of subsite +1. The (*S*)-propranolol molecule, however, has achieved this similar result through binding in a different conformation.

The isopropyl moiety at the end of the (*S*)-propranolol side chain is shifted slightly (∼0.8 Å) relative to that of (*R*)-propranolol (Fig. 3*a*). In both cases the methyl groups fit nicely into a pocket near Ala140, Tyr142 and Trp364 (Pc_Cel7D numbering), but a greater number of van der Waals contacts are made by the (*S*)-enantiomer.

The position of the secondary amino group of the ligand is also similar. The nitrogen is presumably charged in both cases (since the pH of crystallization in each case is 7.0), making it a good match for the acidic residues of the active site. In Tr_Cel7A the amino group hydrogen bonds with an overlapping subset of the catalytic residues (Fig. 2*b*), *i.e.* those equivalent to the nucleophile Glu207 and the acid/base Glu212 (instead of residues 207 and 209). The hydrogen-bonding distance to the nucleophile is also slightly longer than that noted above (2.9 rather than 2.5 Å). For both enzymes, binding of basic compounds is tighter at higher pHs, while the opposite is true for acidic compounds, observations which underline the importance of these electrostatic contributions to binding (Henriksson *et al.*, 2000).

Proceeding along the ligand molecule to its chiral centre (*i.e.* the carbon carrying the alcohol group), the two enantiomers begin to exhibit conformational differences as well as more distinct interactions with the proteins (Fig. 3*a*). In the (*S*)-propranolol complex, the alcohol group points towards the 'bottom' of the active site (Fig. 2*b*), allowing it to hydrogen bond to the catalytic nucleophile Glu212 (corresponding to

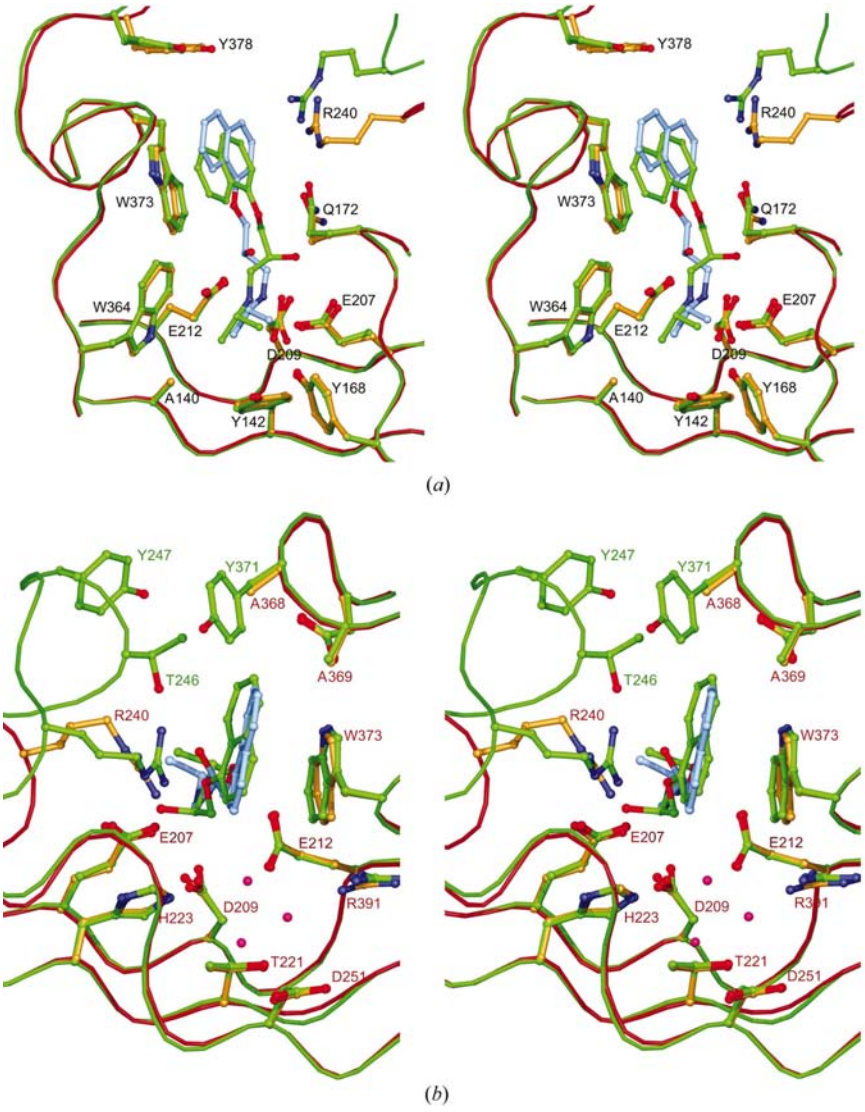

Figure 3
Similarities and differences in ligand docking. (*S*)-propranolol as bound to Tr_Cel7A (green C atoms in ligand and protein) is superimposed on the complex of Pc_Cel7D and (*R*)-propranolol (C atoms are light blue in ligand and gold in protein) and shown in divergent stereo. (*a*) View from 'above' the catalytic cleft showing that the active sites are practically identical around most of the ligand. The residue numbers are for Pc_Cel7D. The isopropyl moieties, pointing downwards in this view, and the secondary amino groups are in similar positions. The rest of the amino-alcohol chains have different conformations and the naphthyl groups are shifted. (*b*) View from the end of the cleft along the bottom of the binding site towards the catalytic residues. Tr_Cel7A (green labels) has a loop (top left) that extends above the active site and which, together with Tyr371 on the opposing loop, encloses the naphthyl moiety of the ligand. In Pc_Cel7D (brown labels) the corresponding loop is shorter and leaves one face of the upper part of the naphthyl exposed to solvent. In both complexes there is room for water molecules between the ligand and the 'bottom' of the binding cleft; some from the Pc_Cel7D–(*R*)-propranolol complex are shown as red spheres. The protein structures were aligned initially by matching residues 207–212 of Pc_Cel7D to 212–217 of Tr_Cel7A; the alignment was improved using a 1.0 Å cutoff. This approach results in an r.m.s. difference of 0.5 Å for 329 C^{α} atoms.

Glu207 in Pc_Cel7D) as well as to a conserved glutamine Gln175 (Gln172 in Pc_Cel7D). In the (*R*)-propranolol complex (Fig. 2*a*), the different configuration forces the chiral carbon 'upwards' by nearly 2 Å (Fig. 3*a*), bringing it into van der Waals contact with the acid/base Glu212 (3.5 Å). The alcohol group then also points 'upwards' and is in contact with, but does not hydrogen bond to, the side chain of Gln172 (3.5 Å). These changes mean that the hydrogen bonds of the ligand with Glu207 and Gln172 are lacking in the complex with the (*R*)-enantiomer. The ether oxygen is also shifted somewhat; it does not make a hydrogen bond in either structure, although in the (*S*)-propranolol complex it does make van der Waals contacts with the side chain of Gln175 (corresponding to Gln172 in Pc_Cel7D).

The naphthyl group of (*R*)-propranolol is stacked onto both rings of Trp373 in Pc_Cel7D, but is tilted slightly relative to the plane of the indole. The separation between the aromatic systems ranges from 3.2 to ∼5 Å. The nearest residue on the opposite side of the naphthyl is Arg240 (with a closest distance of 3.2 Å, between Arg240 NH2 and the edge of one of the rings). The naphthyl group in the Tr_Cel7A structure with (*S*)-propranolol occupies a similar position, although it is rotated and translated slightly (Fig. 3). The differences in position of the corresponding atoms range from 0.9 Å for the carbon to which the ether oxygen is attached to 3.7 Å for the outer edge of the secondary naphthyl ring. This means that in the (*R*)-enantiomer the naphthyl group is buried ∼1 Å deeper in the binding site and overlaps to a larger extent with the tryptophan platform; interactions with Ala369 and Tyr378 equivalents are also absent in the (*S*)-propranolol complex. We also note that the electron density is better for this part in the ligand in the Tr_Cel7A–(*S*)-propranolol complex and that temperature factors for both the ligand and the tryptophan are somewhat lower.

3.4. Implications for enantioseparations using Pc_Cel7D and Tr_Cel7A

The primary goal in the present studies was to investigate the reasons underlying the separation of propranolol enantiomers by Pc_Cel7D and Tr_Cel7A. Unfortunately, we were not able to obtain a structure of Pc_Cel7D in complex with (*S*)-propranolol. A number of attempts to obtain a complex of Tr_Cel7A with (*R*)-propranolol had also failed (Ståhlberg *et al.*, 2001). Given the effects of various conditions on binding of the two enantiomers, it seems possible that we have fortuitously found circumstances that favour extreme enantioselectivity, an idea that we will investigate further.

The available inhibition constants for the two enzymes are summarized in Table 2. (*S*)-Propranolol is bound equally well by both. An inspection of the structures suggests that (*S*)-propranolol would be able to bind in the same mode to Pc_Cel7D as it does to Tr_Cel7A. All of the interacting residues are present and with essentially identical structure; one minor difference is seen for the conformation of the side chain of Arg240, but the end of the side chain that actually makes contact with the ligand is expected to be in an equivalent position.

Table 2
Inhibition constants for propranolol enantiomers.

Enzyme activity on the substrate *p*-nitrophenyl lactopyranoside was assessed by spectroscopic measurements of the release of *p*-nitrophenol. A comparative study of the inhibition of the two enzymes by the enantiomers of propranolol in 10 m*M* sodium acetate buffer pH 5.0 at 298 K was carried out by Henriksson *et al.* (2000). Values in parentheses are those reported by Ståhlberg *et al.* (2001) for Tr_Cel7A under conditions approximating those in the crystallization experiments [100 m*M* 2-(*N*-morpholino)ethanesulfonic acid pH 7.0, 15% monomethyl polyethylene glycol, 10% glycerol].

Enzyme	K_i, (*R*)-propranolol (μ*M*)	K_i, (*S*)-propranolol (μ*M*)
Pc_Cel7D	270	70
Tr_Cel7A	500 (220)	70 (44)

Both enzymes prefer the (*S*)-enantiomer to the (*R*)-form. One main difference between the binding of the (*R*)- and (*S*)-forms in the known structures is that the (*S*)-form's alcohol makes two hydrogen bonds which are not present in the (*R*)-propranolol complex. The equivalent hydroxyl group of the (*R*)-enantiomer only interacts with a water molecule that makes no further interactions with either protein or ligand. The (*S*)-enantiomer also lies slightly deeper in the active site, making more van der Waals interactions in that vicinity. Combined, these provide a structural explanation for why (*S*)-propranolol binds more tightly to both enzymes.

The remaining issue is how to correlate the structural situation with the observation that (*R*)-propranolol binds more tightly to Pc_Cel7D than to Tr_Cel7A. The difference in K_i is small but reproducible and the relative enantioseparation is the same at several different pH values (Henriksson *et al.*, 2000). The structure of the two enzymes near the amino-alcohol side chain of propranolol is essentially identical; the space is very narrow and leaves little room for alternative conformations of this part of the ligand (Fig. 3). Although there is some possibility for sliding of the ligand within the binding site, as illustrated by the complex with (*S*)-propranolol described above, it appears unlikely that such movements are generated by this part of either the ligand or the enzyme. We conclude that the most critical differences must lie in some aspect of the binding to the naphthyl group of propranolol.

The most striking structural difference between the two enzymes is the fact that three of the tunnel-enclosing loops present in Tr_Cel7A are partially deleted in Pc_Cel7D. One of these loops is immediately adjacent to the catalytic site where propranolol binds (Fig. 3*b*). This loop has six extra residues in Tr_Cel7A (inserted between Ala239 and Arg240 in the Pc_Cel7D sequence) that completely enclose the catalytic site. The shorter loop in Pc_Cel7D leaves the active site more exposed to solvent. This change has obvious implications for the binding of the naphthyl moiety. The shape and properties of the proteins are identical around most of this group, *i.e.* on the side facing the tryptophan and the lower part of the binding cleft (Fig. 3*b*). On the other side of the secondary ring, however, the surroundings are quite different. This face will be

covered in Tr_Cel7A, while it will be exposed in Pc_Cel7D. Microcalorimetric and chromatographic studies of Tr_Cel7A have shown that its affinity for beta blockers increases with temperature, suggesting that the binding is an entropy-driven process (Fornstedt *et al.*, 1997; Hedeland, Henriksson *et al.*, 2000; Jönsson *et al.*, 1992). The presence (or absence) of water molecules around the ligand and in the binding site of the protein is thus likely to be an important factor. One possibility is that in the more open Pc_Cel7D more water is freed up by binding the naphthyl group deeper in the cleft. The structural constraints of the binding site of Tr_Cel7A, on the other hand, may lead to a less favourable outcome. Because of the structural differences between the two proteins at this point, it is difficult to predict exactly how the docking of the naphthyl group will differ in Tr_Cel7A; more structural studies will be needed.

The more distantly related *T. reesei* endoglucanase Cel7B (previously called EG 1) has a very similar active site, but the loops that form the tunnel in Tr_Cel7A are much shorter, leading to a completely open cleft (Kleywegt *et al.*, 1997). This enzyme displays very poor enantioselectivity compared with either Pc_Cel7D or Tr_Cel7A (Henriksson *et al.*, 1996), giving additional support to the idea that exact shape of the enzyme in the tunnel/cleft near the active site has a strong influence on the binding of different enantiomers.

The authors are grateful to Dr Gunnar Johansson, Department of Biochemistry, Uppsala University for providing Pc_Cel7D protein, and to Dr Göran Pettersson, Dr Hongbin Henriksson and Dr Roland Isaksson for fruitful discussions. This work was supported by the Swedish Foundation for Strategic Research *via* the Swedish Structural Biology Network (SBNet; IM/JS) and the Glycoconjugates in Biological Systems network (GLIBS; SM), as well as by the Centre for Forest Biotechnology and Chemistry (JS), the Bo Rydins Foundation for Scientific Research (JS), the Swedish Council for Forestry and Agricultural Research (JS) and the Swedish Research Council (SM).

References

Aboul-Enein, H. Y. & Serignese, V. (1997). *Biomed. Chromatogr.* **11**, 47–49.
Barr, B. K., Hsieh, Y. L., Ganem, B. & Wilson, D. B. (1996). *Biochemistry*, **35**, 586–592.
Berman, H. M., Westbrook, J., Feng, Z., Gilliland, G., Bhat, T. N., Weissig, H., Shindyalov, I. N. & Bourne, P. E. (2000). *Nucleic Acids Res.* **28**, 235–242.
Boisset, C., Fraschini, C., Schülein, M., Henrissat, B. & Chanzy, H. (2000). *Appl. Environ. Microbiol.* **66**, 1444–1452.
Brünger, A. T. (1992). *Nature (London)*, **355**, 472–475.
Collaborative Computational Project, Number 4 (1994). *Acta Cryst.* D**50**, 760–763.
Davies, G. J., Wilson, K. S. & Henrissat, B. (1997). *Biochem. J.* **321**, 557–559.
Divne, C., Ståhlberg, J., Reinikainen, T., Ruohonen, L., Pettersson, G., Knowles, J. K., Teeri, T. T. & Jones, T. A. (1994). *Science*, **265**, 524–528.
Divne, C., Ståhlberg, J., Teeri, T. T. & Jones, T. A. (1998). *J. Mol. Biol.* **275**, 309–325.
Eriksson, K. E. & Pettersson, B. (1975). *Eur. J. Biochem.* **51**, 213–218.
Fornstedt, T., Sajonz, P. & Guiochon, G. (1997). *J. Am. Chem. Soc.* **119**, 1254–1264.
French, G. S. & Wilson, K. S. (1978). *Acta Cryst.* A**34**, 517–525.
Gebler, J., Gilkes, N. R., Claeyssens, M., Wilson, D. B., Beguin, P., Wakarchuk, W. W., Kilburn, D. G., Miller, R. C. Jr, Warren, R. A. & Withers, S. G. (1992). *J. Biol. Chem.* **267**, 12559–12561.
Götmar, G., Fornstedt, T., Andersson, M. & Guiochon, G. (2001). *J. Chromatogr. A*, **905**, 3–17.
Haginaka, J. (2000). *J. Chromatogr. A*, **875**, 235–254.
Harris, M. & Jones, T. A. (2001). *Acta Cryst.* D**57**, 1201–1203.
Hedeland, M., Henriksson, H., Backman, P., Isaksson, R. & Pettersson, G. (2000). *Thermochim. Acta*, **356**, 153–158.
Hedeland, M., Nygard, M., Isaksson, R. & Pettersson, C. (2000). *Electrophoresis*, **21**, 1587–1596.
Henriksson, H., Muñoz, I. G., Isaksson, R., Pettersson, G. & Johansson, G. (2000). *J. Chromatogr. A*, **898**, 63–74.
Henriksson, H., Ståhlberg, J., Isaksson, R. & Pettersson, G. (1996). *FEBS Lett.* **390**, 339–344.
Henrissat, B. & Bairoch, A. (1996). *Biochem. J.* **316**, 695–696.
Henrissat, B. & Davies, G. (1997). *Curr. Opin. Struct. Biol.* **7**, 637–644.
Henrissat, B., Teeri, T. T. & Warren, R. A. (1998). *FEBS Lett.* **425**, 352–354.
Isaksson, R., Pettersson, C., Pettersson, G., Jönsson, S., Marle, I., Ståhlberg, J. & Hermansson, J. (1994). *Trends Anal. Chem.* **13**, 431–439.
Jones, T. A., Zou, J.-Y., Cowan, S. W. & Kjeldgaard, M. (1991). *Acta Cryst.* A**47**, 110–119.
Jönsson, S., Schon, A., Isaksson, R., Pettersson, C. & Pettersson, G. (1992). *Chirality*, **4**, 505–508.
Kleywegt, G. J. (1996). *Acta Cryst.* D**52**, 842–857.
Kleywegt, G. J. (1997). *J. Mol. Biol.* **273**, 371–376.
Kleywegt, G. J. & Brünger, A. T. (1996). *Structure*, **4**, 897–904.
Kleywegt, G. J. & Jones, T. A. (1996). *Structure*, **4**, 1395–1400.
Kleywegt, G. J., Zou, J. Y., Divne, C., Davies, G. J., Sinning, I., Ståhlberg, J., Reinikainen, T., Srisodsuk, M., Teeri, T. T. & Jones, T. A. (1997). *J. Mol. Biol.* **272**, 383–397.
Marle, I., Erlandsson, P., Hansson, L., Isaksson, R., Pettersson, C. & Pettersson, G. (1991). *J. Chromatogr.* **586**, 233–248.
Marle, I., Jönsson, S., Isaksson, R., Pettersson, C. & Pettersson, G. (1993). *J. Chromatogr.* **648**, 333–347.
Moews, P. C. & Kretsinger, R. H. (1975). *J. Mol. Biol.* **91**, 201–228.
Moffat, A. C., Jackson, J. V., Moss, M. S. & Widdop, B. (1986). *Clarke's Isolation and Identification of Drugs*, 2nd ed. London: Pharmaceutical Press.
Muñoz, I. G., Ubhayasekera, W., Henriksson, H., Szabó, I., Pettersson, G., Johansson, G., Mowbray, S. L. & Ståhlberg, J. (2001). *J. Mol. Biol.* **314**, 1097–1111.
Murshudov, G. N., Vagin, A. A. & Dodson, E. J. (1997). *Acta Cryst.* D**53**, 240–255.
Murshudov, G. N., Vagin, A. A., Lebedev, A., Wilson, K. S. & Dodson, E. J. (1999). *Acta Cryst.* D**55**, 247–255.
Ståhlberg, J., Divne, C., Koivula, A., Piens, K., Claeyssens, M., Teeri, T. T. & Jones, T. A. (1996). *J. Mol. Biol.* **264**, 337–349.
Ståhlberg, J., Henriksson, H., Divne, C., Isaksson, R., Pettersson, G., Johansson, G. & Jones, T. A. (2001). *J. Mol. Biol.* **305**, 79–93.